# Serveur Académique Lausannois SERVAL serval.unil.ch

# Author Manuscript
## Faculty of Biology and Medicine Publication

This paper has been peer-reviewed but dos not include the final publisher proof-corrections or journal pagination.

Published in final edited form as:

serval
serveur académique lausannois

UNIL | Université de Lausanne
Faculté de biologie et de médecine

**Structure of the extracellular domains of human and xenopus Fn14: Implications in the evolution of TWEAK and Fn14 interactions.**

*Maria Pellegrini[1,2,*], Laure Willen[3], Mai Perroud[3], Dennis Krushinskie[1], Kathy Strauch[1], Hernan Cuervo[1], Eric S. Day[1], Pascal Schneider[3] and Timothy S. Zheng[1]*

[1]Biogen Idec Inc., 14 Cambridge Center, Cambridge, MA, USA. [2]Present address: Dartmouth College, Department of Chemistry, Hanover, NH, USA. [3]Department of Biochemistry, University of Lausanne, Epalinges, Switzerland.

* Address correspondence to: Maria Pellegrini, Dartmouth College, 6128 Burke Hall, Hanover, NH, USA; Phone: +1 603 646 8103; Fax: +1 603 646-3946; E-mail: Maria.Pellegrini@Dartmouth.edu.

RUNNING TITLE:  Structure and Evolution Relationship in Fn14

ABBREVIATIONS: TWEAK, TNF homologue with weak apoptosis inducing activity; Fn14, Fibroblast growth factor-inducible protein 14; CRD, Cysteine-Rich Domain; TACI, Transmembrane Activator and Calcium signal-modulating cyclophilin ligand (CAML)-Interactor; TACI_d2, Second CRD of TACI; BCMA, B cell maturation antigen; APRIL, A Proliferation-Inducing Ligand; BAFF, B cell activation factor of the TNF family; BAFFR, BAFF receptor; PDB, Protein Data Bank; FACS, fluorescence-activated cell sorting; ELISA, enzyme-linked immunosorbent assay; SPR, surface plasmon resonance; HSQC, Heteronuclear Single-Quantum Coherence.

KEYWORDS: Fn14, TWEAK, NMR; TNF; evolution.

Databases: structural data are available in the Protein Data Bank/BioMagResBank databases under the accession codes: **2KMZ**, **2KN0**, **2KN1** and **17237**, **17247**, **17252**

**Abstract**

TWEAK and Fn14 are members of the TNF ligand and receptor superfamilies. Upon observation that xenopus Fn14 cross reacts with human TWEAK, despite its relatively low sequence homology to human Fn14, we set out to examine the conservation in tertiary fold and binding interfaces between the two species. Our results, combining NMR solution structure determination, binding assays, extensive site-directed mutagenesis and molecular modeling, reveal that in addition to the known and previously characterized β-hairpin motif, the helix-loop-helix motif brings an essential contribution to the receptor/ligand binding interface. We further discuss the insight provided by the structural analyses on how the cysteine-rich domains of TNF receptor superfamily may have evolved over time.

## Introduction

TNF (tumor necrosis factor) family ligands and their receptors, to which TWEAK (TNF like weak inducer of apoptosis) and its receptor Fn14 (fibroblast growth factor inducible immediate-early response protein 14) belong, regulate a wide range of biological processes including inflammation, lymphocyte survival and activation, as well as tissue repair and remodeling [1, 2]. Although the TWEAK-Fn14 pathway does not seem to play any obligatory role in tissue development and homeostasis, growing evidence indicates that TWEAK-mediated Fn14 activation constitutes an evolutionarily highly conserved [3-5] physiological response to injury by facilitating tissue regeneration and repair [6, 7]. However, dysregulation of the TWEAK-Fn14 pathway under pathological conditions can contribute to amplification of an excessive inflammatory response, to pathogenic angiogenesis and tissue remodeling, to inhibition of endogenous repair mechanisms, [8] and has been related to aspects of tumor growth and metastasis [9].

Fn14 along with BCMA, BAFFR and TACI is one of the smallest TNF receptors. It contains just a single extracellular cysteine rich domain (CRD), and two nested disulfide bridges, a disulfide bond pattern different from that of BCMA and TACI (Fig. 1) [10]. In the current study, we relate the solution conformations and ligand binding affinities of the soluble ectodomains of human and xenopus Fn14. Despite considerable divergence in their primary sequences, human and xenopus Fn14 adopt a nearly identical overall fold consistent with the observation that both can bind to human TWEAK. The conserved structural motifs, coupled with site-directed mutagenesis of both Fn14 and TWEAK allow us to define the interaction site and to model the interface of the TWEAK/Fn14 complex using the available structures of other TNFRs in complex with their ligands [11-13] and the newly determined solution structure of BCMA.

## Results and discussion

### Evolutionary conservation of TWEAK-Fn14 interactions

Human and xenopus Fn14 (referred to as hFn14 and xeFn14) share only 37% sequence identity overall and 40% in the extracellular domain [14], but share several common features (Fig. 1), including a single extracellular CRD with six identically-spaced cysteine residues that are separated by short stretches of homologous amino acids. To test the role of the conserved residues in interacting with TWEAK we measured the binding of human or xenopus Fn14 to human TWEAK by fluorescence-activated cell sorting (FACS), enzyme-linked immunosorbent assay (ELISA) and surface plasmon resonance (SPR). Figure 2A shows FACS analysis in which we transfected full-length hFn14 or xeFn14 into 293 T cells and measured the binding of Fc-hTWEAK. Similarly, figure 2B shows ELISA results with Fc-hTWEAK titrated on human or xenopus Fn14 coated plates. We observed comparable binding to both species with an $EC_{50}$ of 0.3 nM for Fc-hTWEAK binding to each receptor. The values are in agreement with what recently reported for a conjugated form of human TWEAK binding to hFn14 in human HT1080 and HT29 cells [15]. The high affinity detected for the xeFn14/hTWEAK interaction prompted us to measure the true, monovalent affinity of human and xenopus Fn14 for human TWEAK by SPR. Figure 2, panels C and D, shows the results of the equilibrium binding of monomeric xenopus or human Fn14 respectively to hTWEAK measured by SPR. hFn14 binds to hTWEAK with a $K_D$ = 65 nM (Fig. 2D) while xeFn14 binds to hTWEAK with a $K_D$ = 1.3 $\mu$M (Fig. 2C); a 20-fold lower affinity than hFn14. This difference, which cannot be detected in avidity prone, multivalent-interaction assay formats [16], becomes apparent only when the single-site binding affinity is measured. Importantly, hTWEAK induced similarly robust NF-κB activation when co-transfected with either hFn14 or xeFn14 in 293T cells, indicating that the observed interaction with xeFn14 can yield functional signals (Fig. 2E). Taken together, these data strongly suggests that endogenous interactions between TWEAK and Fn14 were by and large highly conserved during evolution.

### Solution structure of hFn14 and xeFn14 extracellular domains

To understand the structural basis underlying the high level of cross-species conservation of TWEAK - Fn14 interactions, we determined the structure of the extracellular ligand-binding domain of both hFn14 and xeFn14 by NMR (Fig. 3A and B). The solution structure we obtained for hFn14 is in agreement with the published structure [17], with average pairwise rmsds in the structured regions of 0.62 and 0.47 Å (family of 20 structures vs. PDB code **2RPJ** structure 1) and same tertiary arrangement. hFn14 and xeFn14 share strong similarity in the NMR spectral pattern (chemical shifts and NOEs, Fig. S1), which translates to highly similar secondary and tertiary structures (rmsd 1.0 Å over secondary structure regions: residues 40-52, 61-64, backbone atoms, Fig. 3B; numbering as in hFn14). The disulfide pattern of hFn14 was determined using tandem mass spectrometry[10], and was further confirmed by NMR for both hFn14 and xeFn14. Both proteins adopt a nested pattern in the two most C-terminal disulfide bonds, in contrast to the intercalated pattern observed in BCMA and TACI_d2, the two TNFR superfamily members previously thought to be most closely-related to Fn14 (Fig. 1B, 3A and 3C). The highly ordered β-hairpin domains (rmsd 0.24 Å and 0.20Å respectively, for each ensemble of 20 structures of hFn14 and xeFn14), converge to an rmsd of 0.56 Å. This area of the molecule has been previously reported to provide the majority of the interaction interface with the ligand for BCMA and BAFFR, and to be essential for binding in TACI and multi-domain TNF receptors (TNFR1, DR5) [18, 19].

The relative arrangement of the C-terminal lobe of Fn14 proteins (helix1, residues 52-55, loop and helix2, residues 62-69) and the N-terminal β-hairpin is well defined by a number of long range NOEs radiating from the central aromatic residue Phe[63]/xPhe[54] (for simplicity the first residue refers to hFn14 and the "x" residue to the correspondent in xeFn14; NOEs to Ser[41]/xAla[32], Trp[42]/xTyr[33], Ser[43]/xSer[34], Met[50]/xMet[41]). In the case of xeFn14, long-range contacts between the two acidic residues xAsp[53] and xAsp[36] can also be clearly observed. To quantitatively evaluate NOEs and their impact on the final structures we utilized the program QUEEN [20]. The average information, $I_{ave}$, of long range restraints connecting residues in the loop (Phe[63], Gly[66], Cys[67]; xPhe[54], xAsn[57], xCys[58]) to residues in N-terminal region (Ser[41], Ser[43] and xArg[31]- xSer[34]) is 32% and 35% respectively of the total structural information, indicating a dominant

role in the structure. NOEs in the helix2 region have a higher contribution in the dataset for hFn14 than for xeFn14 (a better chemical shift dispersion is observed). Correspondingly helix2 in the human protein is better defined and folds into a more compact coil (Fig. 3B).

The observed structures closely resemble that of TACI_d2 (rmsd 0.52 Å between residues 40-50 of hFn14 and residues 77-87 of TACI_d2, lowest NOE violation structure, PDB code **1XUT**) (Fig. 4A and C).

**Solution structure of BCMA**

The relative orientations of the N- and C-terminal lobes of Fn14 determined by NMR is strikingly different from those of TACI_d2 and especially BCMA as determined by crystallography [12, 13] (Fig. 4). We confirmed that the solution structure of BCMA is highly similar to the crystal structures of BCMA determined previously in complex with BAFF or APRIL [12, 21]; the backbone rmsd over the ordered regions is 1.06 Å (lowest NOE violation structure vs. PDB code **1OQD**). A similar analysis of the NMR restraints (QUEEN) indicates that the relative orientation of the N-and C-terminal lobes is well characterized by long range NOEs which constitute about 19% of the total structural information (sum of $I_{ave}$), involving residues homologous to what observed for Fn14 (Pro$^{34}$, Thr$^{36}$, Tyr$^{40}$, Cys$^{41}$ to Asn$^{11}$, Tyr$^{13}$, Phe$^{14}$).

**Tertiary fold and binding epitopes for single CRD TNFRs**

Overall, the fold of Fn14 is similar to those of BCMA, TACI_d2 and partially BAFFR, with the most striking similarity in the β-hairpin. The conserved DXL motif, located at the tip of the β-hairpin and essential for ligand binding [11, 12] is replaced in Fn14 by an SXDL sequence that we show here to contribute to ligand binding. Whereas the hydrophobic core in h/xeFn14 is very compact (Phe$^{63}$/xPhe$^{54}$ and Met$^{50}$/xMet$^{41}$, surrounded by a small-amino acids garland: Ser$^{41}$/xAla$^{32}$, Ser$^{43}$/xSer$^{34}$, Ser$^{54}$/xVal$^{45}$ and Ser$^{61}$/xSer$^{52}$ , Fig. 3D), the hydrophobic core of TACI_d2, involves a number of bulkier hydrophobic residues including Phe$^{78}$, Ile$^{87}$, Ile$^{92}$ and Pro$^{97}$ [12] (Fig. 4C), causing a tertiary arrangement progressively more open in TACI_d2 and BCMA, ("opened-clamp" vs. "closed-clamp" in Fn14, Fig. 4).

As a functional consequence of the tertiary structure, BCMA and BAFFR engage BAFF (and APRIL) mostly through the β-hairpin interface [13, 21], with no fundamental contribution from residues in the C-terminal helix-loop-helix region. The intermediate conformation in TACI_d2 involves a wider binding surface to APRIL, encompassing the concave face of the molecule (DXL hairpin plus residues in the helix-loop-helix motif) [12]. In the "closed-clamp" conformation seen in both human and xeFn14, the β-hairpin and the helix-loop-helix motifs are in close proximity and define the binding epitope presented to TWEAK (Fig. 4).

**A discontinuous binding epitope: mutagenesis and molecular structure**

Previous studies have concluded that minimal ligand-induced structural changes occur when BAFFR, BCMA or TACI_d2 bind their respective ligands [11-13], an observation confirmed by the present solution structure of BCMA. A model of hFn14 bound to TWEAK was constructed based on the assumptions that a) the structure of free Fn14 and TWEAK-bound Fn14 is similar and b) the region contacted by Fn14 in TWEAK corresponds to that contacted by BAFFR, BCMA and TACI_d2 in BAFF and APRIL. We based our homology model on the available structure of the APRIL-TACI complex (PDB code **1XU1**) [12]. Fn14 contacts TWEAK along a relatively narrow but elongated surface comprising, on one hand, the C-terminal end of the CD loop plus β-strand E of TWEAK, and, on the other hand, the β-hairpin and part of the C-terminal portion of Fn14 .

The molecular model of the TWEAK-Fn14 complex, which takes into account the experimentally determined structure of Fn14, clearly highlights that residues belonging to the two lobes of Fn14 (the β-hairpin and the helix-loop-helix domain) make determinant contributions to the binding interface. Based on the complex structure, selected point mutations were introduced in Fn14 and TWEAK in order to probe potential residues involved in the receptor-ligand interactions. Full-length forms of Fn14 were expressed in 293T cells and stained by FACS with Flag-TWEAK, or with a monoclonal anti-Fn14 antibody (ITEM-4) to control expression levels (Fig. 5A). Leu[46] was deemed important for binding and indeed upon mutation (L46A) binding affinity to TWEAK was reduced, while all other Fn14 mutants

tested bound Flag-TWEAK as efficiently as wild type Fn14 (Fig. 5B). Consequently we introduced a series of double mutations in the hFn14 sequence that combine a residue from the β-hairpin's tip and a residue from the helix-loop helix, expressed them in 293T cells and tested them for binding to hTWEAK. Several double mutants resulted in partial or complete loss of binding to TWEAK: L46A/P59A, L46A/S61A, L46A/D62A and L46A/F63A (Fig 5C). To confirm the importance of the SXDL motif a number of double mutants with both residues within the β-hairpin were also examined. Mutants S43A/L46A, D45A/L46A, D47A/L46A, K48A/L46A almost completely lost the ability to bind to TWEAK (Fig 5C).

Similarly we mapped the TWEAK binding interface, revealing the importance of $Tyr^{176}$ (Y176A completely abolishes binding; Fig. 5D), and the contribution of $Lys^{178}$, $Arg^{190}$ and $Leu^{198}$ (K178A, R190A and L192E all failed to interact with Fn14 L46A, the weakened receptor for TWEAK; Fig. 5E). The residues thus discovered all appear to be involved in specific receptor-ligand interactions and are highlighted in figure 6. For example $Leu^{46}$ on Fn14 interacts with $Leu^{192}$ on TWEAK, $Asp^{47}$-Fn14 at $Lys^{235}$-TWEAK, $Ser^{61}/Asp^{62}$-Fn14 at $Lys^{178}$-TWEAK. $Pro^{59}$, which has a moderate effect on the binding affinity in the double mutant Fn14, may play a structural role or additionally directly participate in binding, similar to the corresponding residue $Pro^{97}$ of TACI_d2 (part of the hydrophobic surface interacting with APRIL). We attribute a structural role also to $Met^{50}$: as part of the hydrophobic core of Fn14 (only 20% of its surface is accessible) it is not predicted to contact TWEAK directly but rather to play a major role in determining the relative orientation of the N- and C-terminal lobes. A similar effect was reported previously for the equivalent position of TACI_d2 ($Ile^{87}$) [12] (Fig. 4C). Several residues showed no contribution to binding (Fig. 5C): $Arg^{56}$, $Arg^{58}$ and $Leu^{65}$ are pointing away from the TWEAK interface in the model and make no or little contacts with TWEAK while $His^{60}$ points toward $Glu^{194}$ and $Phe^{195}$ of TWEAK.

Within the series of single mutant hFn14 constructs, the result that each mutation taken alone did not disrupt (or only reduced, e.g. L46A) ligand binding indicates that none of these mutations resulted in

gross unfolding or intracellular retention of hFn14. It is noteworthy that our results are in contrast with a previous report indicating that the D62A mutation totally prevented the secretion of Fn14 protein and several single point mutations disrupted binding[22]. The secretion of soluble D62A mutant may be affected by the use of full length human Fn14 in this study, versus a murine sequence of the sole extracellular domain of Fn14 fused to murine Fc and a Myc tag. We also tested mutations in neighboring amino acids, S61A and F63A, which yielded Fn14 mutants able to bind TWEAK. In addition, the binding assay modalities were largely different: binding affinities in this study were compared by FACS analysis on cells expressing the described Fn14 mutants with increasing Flag-TWEAK concentrations (upward of 10 μg/ml), where the study reported in [22] measured binding affinity at two concentrations of purified receptors to TWEAK immobilized on a solid surface and the weakest detected binding was reported as a $K_D$ of 71nM. To confirm correct folding of the mutant proteins, a representative double mutant, hFn14(L46A, R58A), was expressed and purified and examined by $^1$H, $^{15}$N-HSQC NMR. The protein spectrum (Fig. S2) closely tracks with the one of wild type hFn14, with chemical shifts perturbations corresponding only to the sites adjacent to the mutated residues as expected, indicating the wild type and mutant proteins are similarly folded.

Taken together, our data indicate that the Fn14-TWEAK interaction involves elements from the β-hairpin as well as from the helix-loop-helix motif. The observation that single point mutations are well tolerated seems to indicate that the multiple sites of this non-contiguous interaction interface may contribute substantially to the energy of binding, which should be taken into account for the development of low molecular weight molecules aimed at modulating the TWEAK-Fn14 interaction.

**Fn14: the evolutionary perspective**

The TNF superfamilies of ligands and receptors have expanded considerably during evolution, from a single pair in drosophila (Eiger-Wengen) to more than twenty in human, as higher organisms relied more and more on these ligand/receptor interactions for controlling cell fate decisions. The evolutionary origin

and diversification of these pairs is however incompletely understood. In the current study, we describe

that the interface between the TNF ligand TWEAK and its cognate receptor Fn14 has been conserved.

Although it may seem remarkable that xenopus Fn14 cross-reacts with human TWEAK, inter-species

cross reactivity is not uncommon in the TNF family: 72% of the TNF ligands and receptors cross-react

between human and mouse [23], human BAFF binds to chicken BAFFR [24], chicken BAFF binds to

human BCMA [25], and mammalian EDA is even active in fishes [26]. The strong structural similarity

that we observe between human and xenopus Fn14 despite divergent primary sequences is probably due

to the presence of a structural core stabilized by disulfide bonds, as shown previously for other protein

families [27, 28].

Most TNF receptor family members, such as TNFR1, TNFR2 and Fas, contain three or four cystein-rich

domains, usually composed of A and B modules (for a classification see [2]), suggesting that these

receptors may have arisen by exon duplication of an ancestral cystein-rich domain such as that found in

Wengen in the Drosophila [29] (Fig. 1B). The relatively recent identification of single CRD receptors in

mammals raised the intriguing possibility that they could represent the ancestral molecules from which

multi-CRD mammalian TNF receptors have evolved [12]. The TWEAK-Fn14 pathway may be one of the

most 'ancient' from the perspective of evolution. Indeed, the other two single-CRD TNF receptors

BAFFR and BCMA regulate B cell function in vertebrates only, whereas an Fn14-like sequence with

perfectly conserved inter-cysteine spacing and exon-intron boundaries is found in the protochordate

*Branchiostoma floridae* (Fig. 1A). This suggests that the origin of the TWEAK - Fn14 pathway preceded

vertebrate evolution and the development of adaptive immunity.

The structure of Fn14 allows formulating a hypothesis regarding the evolutionary relationship between

modules differing in their patterns of disulfide bridges. Although the A1-C2 cysteine-bridging pattern that

we describe in both human and xenopus Fn14 (the two C2 disulfides are nested) contrasts with the A1-D2

pattern of BCMA and TACI (intercalated disulfides), we find that the three dimensional structure of Fn14

could accommodate the A1-D2 disulfide pattern with only minor structural adjustments (Fig. 3C),

suggesting that a certain level of 'ambiguity' in disulfide linkage formation may have existed in the

primordial single CRD TNF receptor, and that this flexibility may have accounted for the emergence of different modules found in mammalian TNF receptors. Similarly a swapping of disulfide paring has been reported to produce bioactive disulfide bond isomers of epidermal growth factor (EGF)-like domains [30].

## Materials and Methods

### Protein preparation

Soluble Flag-tagged human TWEAK (Flag-hTWEAK) or Fc-hTWEAK (residues 106-249; a fusion protein between the Fc portion of human IgG1 and the TNF homology domain of hTWEAK) were generated and characterized as previously described [23]. Full length, untagged human Fn14 was cloned into the mammalian expression vector PCR3 (Life Technologies, Grand Island, NY, USA). Point mutations were introduced by conventional PCR-based methods in full-length Fn14 and hTWEAK, and the resulting plasmids were sequenced on both strands. His-tagged hTWEAK (His-hTWEAK, residues 106-249) and the soluble ectodomains of human Fn14 (residues 28-80) and xenopus Fn14 (residues 23-72) fused to Myc and His tags were cloned and expressed in *Pichia pastoris* according to protocols previously described [31]. The molecular weight of hFn14 as determined by MS spectrometry was 7617 Da, matching the oxidized state for all six cysteine residues and no post-translational modification [10]. Uniformly $^{15}N$ labeled hFn14 and xeFn14 for NMR studies were prepared from cultures supplemented with $(^{15}NH_4)_2SO_4$ following published procedures [32]. Additional forms of soluble Fn14 used in this study included Fc-hFn14 and Fc-xeFn14 (CHO or 293T mammalian cells). The L46A, R58A mutant of hFn14 was initially cloned in a pQE vector (Qiagen) and subject to PCR-based site directed mutagenesis to introduce A46 and A58. It was subsequently subcloned in a modified pET32b vector (Novagen, EMD Millipore, Billerica, MA, USA) between the BamHI and XhoI restriction sites, as a $His_6$-thioredoxin fusion protein containing a tobacco etch virus (TEV) cleavage site and expressed and purified from E. Coli BL21 Star (DE3) (Life Technologies) as in [33]. The last purification step of the cleaved hFn14(L46A,R58A) consisted in size exclusion chromatography (GE Healthcare Biosciences, Pittsburgh, PA, USA, Superdex Peptide 10/300GL), were the protein eluted at the expected mass for a monomeric species. The protein was characterized by SDS-PAGE and $^{1}H,^{15}N$ NMR spectroscopy.

The cysteine-rich domain of human BCMA (2-50) was synthesized by solid phase peptide synthesis (supplementary material).**ELISA Assay**

Microtiter plates were coated with hFn14 or xeFn14 at 10 μg/ml in 100 mM Na-Carbonate buffer, pH 9.2, and then blocked with ELISA buffer (phosphate buffered saline - PBS: 10 mM phosphate, 137 mM NaCl, 2.7 mM KCl, pH 7.4 - 5% non-fat dry milk, 0.05% Tween-20). Plates were washed with wash buffer (PBS, 0.05% Tween-20) and the indicated concentrations of Fc-hTWEAK in ELISA buffer were added for 1 h at room temperature. Plates were washed and bound Fc-hTWEAK was detected by adding horseradish peroxidase-labeled goat anti-human IgG (Fc specific) (Jackson ImmunoResearch Laboratories, Inc., West Grove, PA, USA) at a dilution of 1:1000 in ELISA buffer for 1 hour at room temperature. Plates were developed with TMB substrate (Pierce, Rockford, IL, USA), the reaction was stopped by addition of 2 N $H_2SO_4$ and absorbance was read at 450 nm. $EC_{50}$ values were determined from an empirical 4-parameter fit to the data:

$$y = (a((bx)^c)/(1+((bx)^c)))+d$$

where:  a = upper asymptote
        b = midpoint ($EC_{50}$)
        c = slope of linear part of curve
        d = lower asymptote

**Cell surface binding analysis**

293T cells were transiently transfected by the calcium phosphate precipitation method with plasmids containing full-length wild type human or xeFn14 cDNAs, together with an EGFP expression plasmid [34]. Cells were harvested 24 hours post transfection and stained with varying amounts of Fc-hTWEAK, followed by FITC- or PE-conjugated goat anti-human Fc secondary antibodies. This allowed semi-quantitative estimation of apparent $K_D$'s of binding between Fc-hTWEAK and hFn14 or xeFn14 expressed on the cell surface. Alternatively, 293T cells were co-transfected by the calcium phosphate method with plasmids encoding EGFP and human Fn14 (wild type, or with the indicated single or double mutations). Cells were stained 48 h post-transfection with 50 $\mu$l of Flag-hTWEAK (wild type or mutants) at the indicated concentrations, followed by biotinylated anti-Flag M2 antibody (Sigma-Aldrich, St. Louis, MO, USA) and PE-coupled streptavidin. Cells were also stained with biotinylated ITEM-4 (anti-Fn14 monoclonal antibody), followed by PE-coupled streptavidin. The mean fluorescence intensity of

Flag-hTWEAK staining was measured on cells expressing intermediate levels of EGFP (fluorescence intensity of 100-1000) and was normalized to the level of Fn14 expression measured with ITEM-4.

**Surface Plasmon Resonance Assay**

All Experiments were performed using a Biacore 3000 instrument (GE Healthcare). His-hTWEAK [16] was immobilized on a CM5 sensorchip as described [35]. Soluble, monomeric human or xenopus Fn14 was diluted in Biacore assay buffer (Biacore buffer + 0.05% BSA) to the indicated concentrations and injected over the TWEAK derivatized or control surface, at a flow rate of 50 μl/min. The TWEAK surface was regenerated with 2 x 30 s injections of 10 mM $H_3PO_4$. In all cases binding to the underivatized chip was negligible. Affinity was determined by fitting plots of the response value where binding has come to equilibrium ($R_{eq}$) versus concentration to a hyperbolic single-site binding equation [28].

**NF-kB luciferase assay**

293T cells were plated at $10^4$ cells/well in 96 well plates in 100 $\mu$l DMEM supplemented with 10% FCS. Two days later, plasmid mixes were prepared in one volume DMEM without supplement, mixed with 0.07 volume of Polyfect (Qiagen) for 5 min, diluted with 5 volumes of DMEM, 10% FCS and distributed (25 $\mu$l) on cells in 50 $\mu$l fresh complete medium. Each well received hFn14 or xeFn14 plasmids (20 ng and 3-fold dilutions), ± 4 ng of huTWEAK plasmid and with 7.5 ng each of NF-κB firefly luciferase, renilla luciferase an EGFP plasmids, with empty vector to get 70 ng of plasmid per well. After 48 h, cells were washed, lysed and assayed for firefly and renilla luciferase using a dual reporter luciferase assay (Promega). Firefly luciferase activity was normalized to that of renilla luciferase. NF-kB activation was expressed as fold increase relative to signals obtained in cells transfected without Fn14.

**NMR Spectroscopy**

NMR samples typically consisted of 500-700 $\mu$M $^{15}$N-xeFn14, $^{15}$N-hFn14 or hFn14, in PBS (pH 7.4), 5% $D_2O$. 900 $\mu$M BCMA was dissolved in 10 mM phosphate buffer, pH 6.0, 0.02% $NaN_3$, 5% $D_2O$. NMR spectra were acquired on a Bruker Avance 600 spectrometer equipped with a triple resonance CryoProbe

or TXI probe, at 10-45°C. $^{1}H$ and $^{15}N$ assignments were obtained using three-dimensional $^{15}N$-edited NOESY-HSQC (100ms) and TOCSY-HSQC experiments [36] (64, 200 and 1024 complex points in the $^{15}N$ and $^{1}H$ dimensions) and two-dimensional homonuclear experiments: TOCSY, NOESY (90ms), double quantum filtered-COSY [37]. All NMR data were processed using TOPSPIN (version 1.3, Bruker-Biospin) and analyzed using Sparky [38].

## Structure Calculation

Complete proton and nitrogen resonances assignment was obtained following previously described procedures [39]. Distance restraints were derived from the 3D $^{1}H$-$^{15}N$ edited NOESY and 2D $^{1}H$-$^{1}H$ NOESY experiments, with mixing times varying between 80 and 100 ms. For each protein, 100 structures were calculated using the torsion angle simulated annealing protocol of CNX (version 2002, Accelrys Inc., San Diego, CA, USA) using standard parameters [40], and the 20 structures with lowest total energy were chosen for analysis. The residues in the Myc-His tag were excluded from the structure calculation. The quality of the structures was analyzed using VADAR [41] , and the experimental NMR restraints were quantitatively evaluated using QUEEN [20] (calculation of the unique information, $I_{uni}$, and average information content sampled throughout the complete dataset, $I_{ave}$, over 25 iterations, of each restraint). The structures were visualized with Chimera [42].

## Disulfide bond determination

Disulfide-bond assignments for all three structures were confirmed by NMR utilizing to the method of Klaus et al. [43], which determines the most likely pattern of disulfide bonds based on the calculation of all possible distances between Cβ of cysteine residues involved in disulfide bonds within the initial family of NMR structures (calculated in absence of explicit S-S bonds definitions). To investigate the consequences of disulfide swapping a set of structures with the alternative disulfide configuration was calculated as well.

## Molecular Modeling of TWEAK-Fn14 Interactions

The model of TWEAK was generated by template forcing homologous sequence regions (as generated by BLAST [44]) to the three-dimensional structure of APRIL (PDB entry **1XU1**) [12] with InsightII (Accelrys). The model of the TWEAK trimer and the structure of Fn14 were superimposed respectively on the crystal structure of APRIL and the bound second CRD domain of TACI (TACI_d2) (PDB entry **1XU1**) [12] using InsightII. The complex was then subjected to extensive energy minimization (steepest descents followed by the quasi-Newton-Raphson method, VA09a until the derivatives were less than 0.5 kcal/mol Å, CVFF91 forcefield ), first with the NMR distance constraints applied  to maintain the Fn14 structure (force constant of 100 kcal mol$^{-1}$ Å$^{-2}$), and then again with no constraints, allowing the complex to relax.

**Acknowledgements**

**References**

1.      Locksley RM, Killeen N & Lenardo MJ (2001) The TNF and TNF receptor superfamilies: integrating mammalian biology. *Cell* 104, 487-501.
2.      Bodmer JL, Schneider P & Tschopp J (2002) The molecular architecture of the TNF superfamily. *Trends Biochem Sci* 27, 19-26.
3.      Zhang JX, Sang M, Li JF, Zhao W, Ma HW, Min C, Hu YL, Du MX & Zhang SQ (2011) Molecular structure and characterization of the cytokine TWEAK and its receptor Fn14 in bovine. *Vet Immunol Immunopathol* 144, 238-246.
4.      Zhang JX, Sang M, Zhao W, Ai HX, Shui Y, Li JF, Song R & Zhang SQ (2010) Molecular characterization of the canine cytokine TWEAK (CD255) and its receptor, Fn14 (CD266). *Vet Immunol Immunopathol* 137, 172-175.
5.      Shui Y, Guan ZB & Zhang SQ (2008) Molecular characterization of cytokine TWEAK and its receptor Fn14 in pig (Sus scrofa). *Vet Immunol Immunopathol* 126, 396-402.
6.      Winkles JA (2008) The TWEAK-Fn14 cytokine-receptor axis: discovery, biology and therapeutic targeting. *Nat Rev Drug Discov* 7, 411-425.
7.      Burkly LC, Michaelson JS, Hahm K, Jakubowski A & Zheng TS (2007) TWEAKing tissue remodeling by a multifunctional cytokine: role of TWEAK/Fn14 pathway in health and disease. *Cytokine* 40, 1-16.
8.      Burkly LC, Michaelson JS & Zheng TS (2011) TWEAK/Fn14 pathway: an immunological switch for shaping tissue responses. *Immunol Rev* 244, 99-114.
9.      Michaelson JS & Burkly LC (2009) Therapeutic targeting of TWEAK/Fnl4 in cancer: exploiting the intrinsic tumor cell killing capacity of the pathway. *Results Probl Cell Differ* 49, 145-160.
10.     Foley SF, Sun Y, Zheng TS & Wen D (2008) Picomole-level mapping of protein disulfides by mass spectrometry following partial reduction and alkylation. *Anal Biochem* 377, 95-104.
11.     Gordon NC, Pan B, Hymowitz SG, Yin J, Kelley RF, Cochran AG, Yan M, Dixit VM, Fairbrother WJ & Starovasnik MA (2003) BAFF/BLyS receptor 3 comprises a minimal TNF receptor-like module that encodes a highly focused ligand-binding site. *Biochemistry* 42, 5977-5983.
12.     Hymowitz SG, Patel DR, Wallweber HJ, Runyon S, Yan M, Yin J, Shriver SK, Gordon NC, Pan B, Skelton NJ, Kelley RF & Starovasnik MA (2005) Structures of APRIL-receptor complexes: like BCMA, TACI employs only a single cysteine-rich domain for high affinity ligand binding. *J Biol Chem* 280, 7218-7227.
13.     Kim HM, Yu KS, Lee ME, Shin DR, Kim YS, Paik SG, Yoo OJ, Lee H & Lee JO (2003) Crystal structure of the BAFF-BAFF-R complex and its implications for receptor activation. *Nat Struct Biol* 10, 342-348.
14.     Brown SA, Richards CM, Hanscom HN, Feng SL & Winkles JA (2003) The Fn14 cytoplasmic tail binds tumour-necrosis-factor-receptor-associated factors 1, 2, 3 and 5 and mediates nuclear factor-kappaB activation. *Biochem J* 371, 395-403.

15.     Fick A, Lang I, Schafer V, Seher A, Trebing J, Weisenberger D & Wajant H (2012) Studies of binding of tumor necrosis factor (TNF)-like weak inducer of apoptosis (TWEAK) to fibroblast growth factor inducible 14 (Fn14). *J Biol Chem* 287, 484-495.

16.     Day ES, Cachero TG, Qian F, Sun Y, Wen D, Pelletier M, Hsu YM & Whitty A (2005) Selectivity of BAFF/BLyS and APRIL for binding to the TNF family receptors BAFFR/BR3 and BCMA. *Biochemistry* 44, 1919-1931.

17.     He F, Dang W, Saito K, Watanabe S, Kobayashi N, Guntert P, Kigawa T, Tanaka A, Muto Y & Yokoyama S (2009) Solution structure of the cysteine-rich domain in Fn14, a member of the tumor necrosis factor receptor superfamily. *Protein Sci* 18, 650-656.

18.     Banner DW, D'Arcy A, Janes W, Gentz R, Schoenfeld HJ, Broger C, Loetscher H & Lesslauer W (1993) Crystal structure of the soluble human 55 kd TNF receptor-human TNF beta complex: implications for TNF receptor activation. *Cell* 73, 431-445.

19.     Cha SS, Sung BJ, Kim YA, Song YL, Kim HJ, Kim S, Lee MS & Oh BH (2000) Crystal structure of TRAIL-DR5 complex identifies a critical role of the unique frame insertion in conferring recognition specificity. *J Biol Chem* 275, 31171-31177.

20.     Nabuurs SB, Spronk CA, Krieger E, Maassen H, Vriend G & Vuister GW (2003) Quantitative evaluation of experimental NMR restraints. *J Am Chem Soc* 125, 12026-12034.

21.     Liu Y, Hong X, Kappler J, Jiang L, Zhang R, Xu L, Pan CH, Martin WE, Murphy RC, Shu HB, Dai S & Zhang G (2003) Ligand-receptor binding revealed by the TNF family member TALL-1. *Nature* 423, 49-56.

22.     Brown SA, Hanscom HN, Vu H, Brew SA & Winkles JA (2006) TWEAK binding to the Fn14 cysteine-rich domain depends on charged residues located in both the A1 and D2 modules. *Biochem J* 397, 297-304.

23.     Bossen C, Ingold K, Tardivel A, Bodmer JL, Gaide O, Hertig S, Ambrose C, Tschopp J & Schneider P (2006) Interactions of tumor necrosis factor (TNF) and TNF receptor family members in the mouse and human. *J Biol Chem* 281, 13964-13971.

24.     Schneider K, Kothlow S, Schneider P, Tardivel A, Gobel T, Kaspers B & Staeheli P (2004) Chicken BAFF--a highly conserved cytokine that mediates B cell survival. *Int Immunol* 16, 139-148.

25.     Kothlow S, Morgenroth I, Graef Y, Schneider K, Riehl I, Staeheli P, Schneider P & Kaspers B (2007) Unique and conserved functions of B cell-activating factor of the TNF family (BAFF) in the chicken. *Int Immunol* 19, 203-215.

26.     Colosimo PF, Hosemann KE, Balabhadra S, Villarreal G, Jr., Dickson M, Grimwood J, Schmutz J, Myers RM, Schluter D & Kingsley DM (2005) Widespread parallel evolution in sticklebacks by repeated fixation of Ectodysplasin alleles. *Science* 307, 1928-1933.

27.     Panchenko AR, Wolf YI, Panchenko LA & Madej T (2005) Evolutionary plasticity of protein families: coupling between sequence and structure variation. *Proteins* 61, 535-544.

28.     Fass D (2012) Disulfide bonding in protein biophysics. *Annu Rev Biophys* 41, 63-79.

29.     Kanda H, Igaki T, Kanuka H, Yagi T & Miura M (2002) Wengen, a member of the Drosophila tumor necrosis factor receptor superfamily, is required for Eiger signaling. *J Biol Chem* 277, 28372-28375.

30.     Sampoli Benitez BA & Komives EA (2000) Disulfide bond plasticity in epidermal growth factor. *Proteins* 40, 168-174.

31.     Cachero TG, Schwartz IM, Qian F, Day ES, Bossen C, Ingold K, Tardivel A, Krushinskie D, Eldredge J, Silvian L, Lugovskoy A, Farrington GK, Strauch K, Schneider P & Whitty A (2006) Formation of virus-like clusters is an intrinsic property of the tumor necrosis factor family member BAFF (B cell activating factor). *Biochemistry* 45, 2006-2013.

32.     Wood MJ & Komives EA (1999) Production of large quantities of isotopically labeled protein in Pichia pastoris by fermentation. *Journal of Biomolecular Nmr* 13, 149-159.

33.     Rushe M, Silvian L, Bixler S, Chen LL, Cheung A, Bowes S, Cuervo H, Berkowitz S, Zheng T, Guckian K, Pellegrini M & Lugovskoy A (2008) Structure of a NEMO/IKK-associating domain reveals architecture of the interaction site. *Structure* 16, 798-808.

34.     Schneider P (2000) Production of recombinant TRAIL and TRAIL receptor: Fc chimeric proteins. *Methods Enzymol* 322, 325-345.

35.     Day ES, Cote SM & Whitty A (2012) Binding Efficiency of Protein-Protein Complexes. *Biochemistry*.

36.     Talluri S & Wagner G (1996) An optimized 3D NOESY-HSQC. *J Magn Reson B* 112, 200-205.

37.     Wuthrich K (1986) *NMR of Proteins and Nucleic Acids* John Wiley, New York.

38.     Goddard TD & Kneller DG (2001) Sparky 3.0. *University of California, San Francisco*.

39.     Piserchio A, Pellegrini M, Mehta S, Blackman SM, Garcia EP, Marshall J & Mierke DF (2002) The PDZ1 domain of SAP90. Characterization of structure and binding. *J Biol Chem* 277, 6967-6973.

40.     Stein EG, Rice LM & Brunger AT (1997) Torsion-angle molecular dynamics as a new efficient tool for NMR structure calculation. *J Magn Reson* 124, 154-164.

41.     Willard L, Ranjan A, Zhang HY, Monzavi H, Boyko RF, Sykes BD & Wishart DS (2003) VADAR: a web server for quantitative evaluation of protein structure quality. *Nucleic Acids Research* 31, 3316-3319.

42.     Pettersen EF, Goddard TD, Huang CC, Couch GS, Greenblatt DM, Meng EC & Ferrin TE (2004) UCSF Chimera--a visualization system for exploratory research and analysis. *J Comput Chem* 25, 1605-1612.

43.     Klaus W, Broger C, Gerber P & Senn H (1993) Determination of the disulphide bonding pattern in proteins by local and global analysis of nuclear magnetic resonance data. Application to flavoridin. *J Mol Biol* 232, 897-906.

44.     Altschul SF, Gish W, Miller W, Myers EW & Lipman DJ (1990) Basic local alignment search tool. *J Mol Biol* 215, 403-410.

**Supplementary material**

Figure S1: 2D NOESY spectra of hFn14 and xeFn14. Figure S2: $^1$H,$^{15}$N HSQC spectra of hFn14(28-80) and hFn14(L46A,R58A). Methods for the synthesis of BCMA.

**Table 1.** Restraints and statistics for the ensemble of 20 structures of hFn14, xeFn14 and BCMA

|  | hFn14 | xeFn14 | BCMA |
|---|---|---|---|
| NOE restraints | 230 | 218 | 279 |
| intraresidue | 79 | 56 | 78 |
| sequential | 89 | 81 | 100 |
| medium range $1 < |i - j| < 5$ | 28 | 31 | 45 |
| long range $|i - j| \geq 5$ | 34 | 50 | 56 |
| Rms deviation from experiment | | | |
| NOE constraints (Å) | 0.015 | 0.035 | 0.060 |
| Rms deviation from idealized geometry | | | |
| bonds (Å) | 0.002 | 0.003 | 0.005 |
| angles (deg) | 0.3 | 0.4 | 0.7 |
| Ramachandran analysis[a] | | | |
| most favored regions (%) | 56.3±6.7 | 61.2±5.0 | 56.0±4.5 |
| additionally allowed regions (%) | 34.2±5.7 | 34.0±5.9 | 30.8±4.5 |
| generously allowed regions (%) | 5.8±3.4 | 3.1±2.3 | 8.9±2.4 |
| disallowed regions (%) | 0.2±0.7 | 0.1±0.4 | 0.2±0.6 |
| Average pairwise rms deviations (Å) | | | |
| $Ser^{40}/xPro^{31}$ to $Cys^{67}/xCys^{58}$ | 0.747 | 0.760 | |

[a] VADAR was used to assess the stereochemical quality of the structures

**Figure Legends**

**Figure 1.** Sequence alignment of Fn14 and other small TNF receptors. A: Sequence alignment of Fn14 from human (*Homo sapiens*), mouse (*Mus musculus*), frog (*Xenopus laevis*), fish (*Gasterosteus aculeatus*) and a protochordate (*Branchiostoma floridae*). Conserved residues in the extracellular domain are shaded. Numbering corresponds to the human sequence. TMD: transmembrane domain. TRAF: consensus TRAF binding site. Exon boundaries, when known, are indicated. B: Sequence alignment of the central portion of the extracellular domains of single-CRD TNF receptors and of TNFR1. The elements of secondary structure (β-sheets in green, α-helices in red) are indicated, as well as the disulfide bonds. Residues on purple background were experimentally shown to participate in ligand binding (for Fn14, BCMA, TACI and BAFFR) or to contact the ligand in the ligand-receptor complex (TNFR1). The module composition of the CRD is shown on the right. dWengen: Drosophila Wengen.

**Figure 2.** Cross-species binding of Fn14 to human TWEAK. A: 293 T cells were transiently transfected with the indicated amount of plasmids encoding full-length hFn14 or xeFn14, stained with Fc-hTWEAK at the indicated concentrations, and analyzed by FACS. MFI: mean fluorescence intensity. B: ELISA assay. Immobilized hFn14 and xeFn14 binding to Fc-hTWEAK and detected with anti-human Fc secondary reagents. A 4-parameter equation fitting yielded an apparent $EC_{50}$ of 0.3 nM. C, D: The binding of monomeric Fn14 (in solution) to immobilized trimeric His-hTWEAK on a Biacore chip. The plot of the signal achieved at equilibrium ($R_{eq}$) as a function of the xeFn14 (C) or hFn14 (D) concentration was fitted to a single site binding model as described in Materials and Methods. E: Induction of NF-κB-luciferase reporter activity in 293T cells transfected with varying amounts of xeFn14 or hFn14 plasmids, in the presence or absence of a fixed amount of co-transfected TWEAK. NF-κB activity is expressed as a fold increase relative to cells transfected without Fn14.
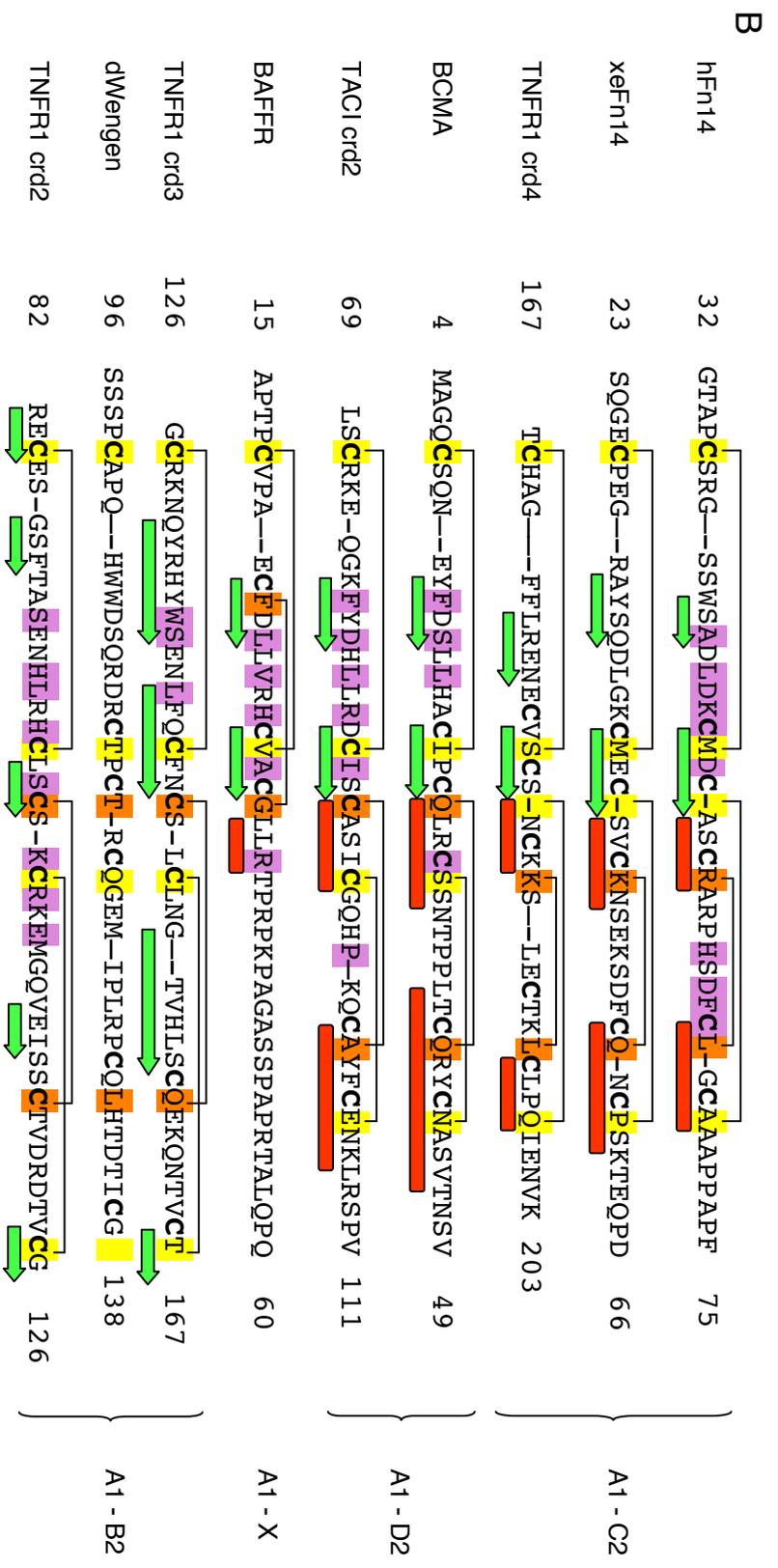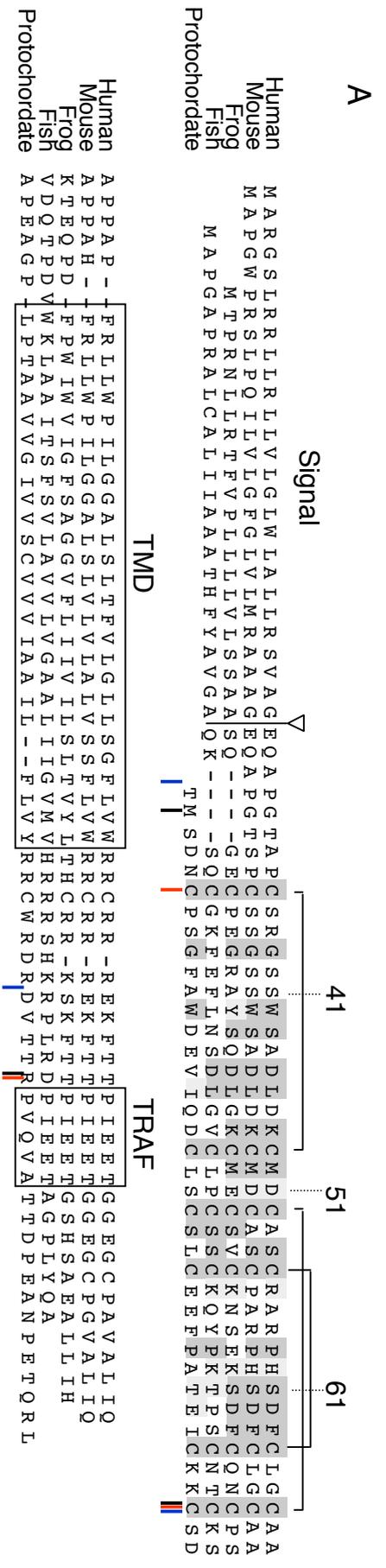
**Figure 3.** NMR solution structure of human and xenopus Fn14. A: Superposition of 20 low energy NMR-derived structures of hFn14 (backbone atoms 36-67). The three disulfide bridges are shown in yellow ball-and-sticks for one of the structures. The boundaries of the A1 and C2 structural modules are indicated by brackets. B: Superposition of low energy structures of hFn14 (gray) and xeFn14 (brick), displayed as ribbons. Residues 36, 40-52 and 61-64 of hFn14 and corresponding residues of xeFn14 were used in the superposition. C: Top view of hFn14 with cysteines highlighted in yellow ball-and-sticks. The arrows indicate changes in disulfide connectivity that would be required to swap from nested to intercalated disulfide bridges in the C2 module. D: The hydrophobic core of hFn14 is constituted of $Phe^{63}$ and $Met^{50}$ (carbon atoms in green), and is surrounded by small amino acids ($Ser^{41}$, $Ser^{43}$, $Ser^{54}$ and $Ser^{61}$, carbon atoms in sky blue). Protons are colored white, oxygens red and sulfur yellow.

**Figure 4.** Comparison of the structural features of hFn14 with BCMA, TACI_d2 and BAFFR. Selected residues are displayed as sticks: in green, residues in the hydrophobic core; in blue, residues relevant for binding in the β-hairpin and helix2. The conserved aromatic is shown in sky blue and disulfides bridges in yellow. Corresponding residues are displayed in the same coloring scheme in panels A-D. A: NMR structure of hFn14. B: NMR structure of hBCMA determined in this study. $Tyr^{13}$ that fulfills a similar structural role as Fn14's $Phe^{63}$ is shown. C: NMR structure of hTACI_d2 (PDB code **1XUT**). D: Crystal structure of hBAFFR (PDB code **1OQE**). Structures shown in panels A to D were first superimposed on their β-hairpins. Note that the N- and C-terminal domains adopt different relative orientations in Fn14 than in BCMA and TACI_d2, which may allow engagement of different epitopes in ligand binding.
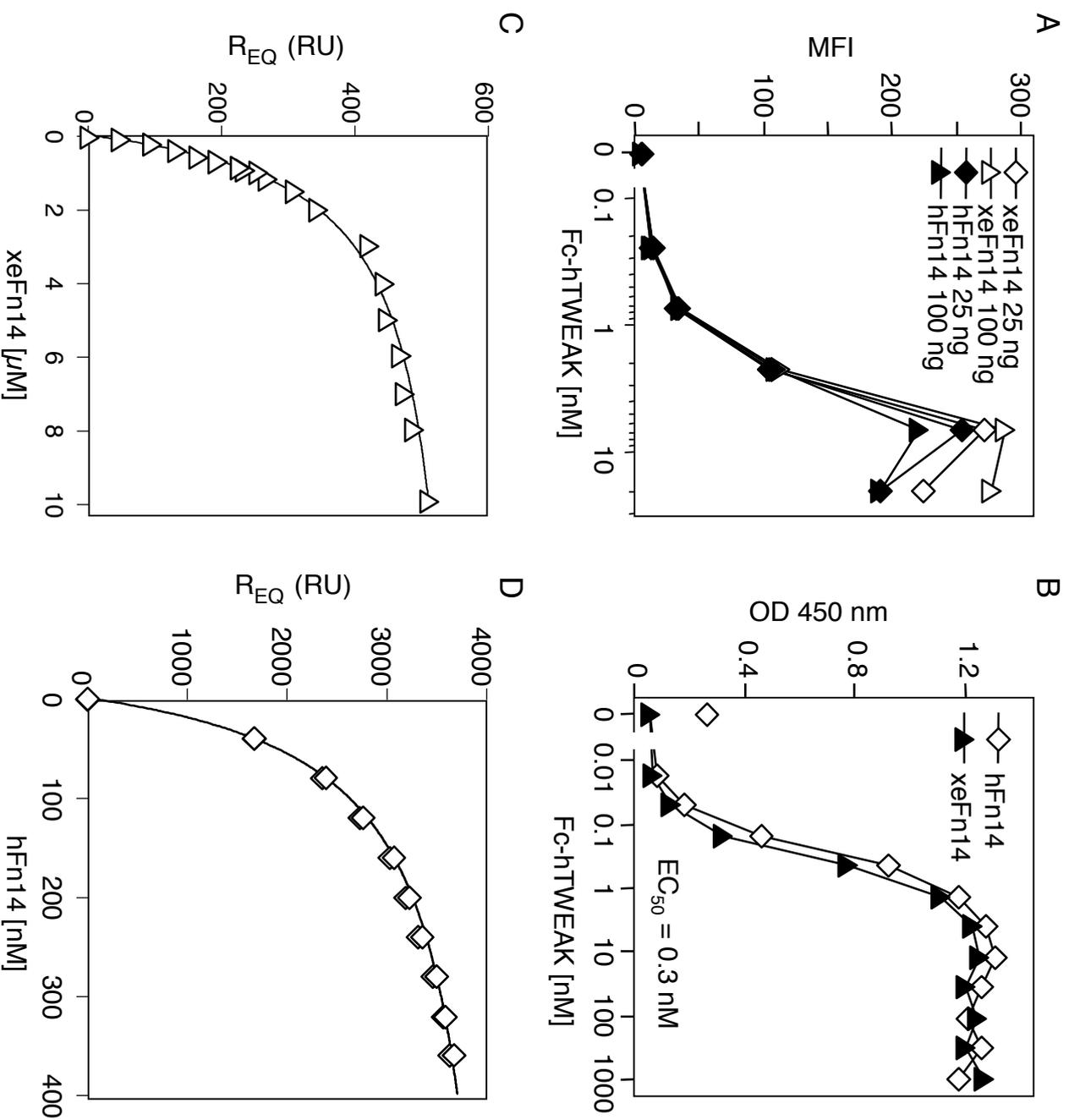
**Figure 5.** Mutagenesis of Fn14 and TWEAK. A: The indicated full-length forms of wild type or mutant Fn14 were expressed in 293T cells and stained by FACS with Flag-TWEAK at the indicated concentrations (for Flag-TWEAK, 1 $\mu$g/ml corresponds to 50 nM), or with a monoclonal anti-Fn14 antibody (ITEM-4) as an expression control. B: The binding of wild type TWEAK to wild type and
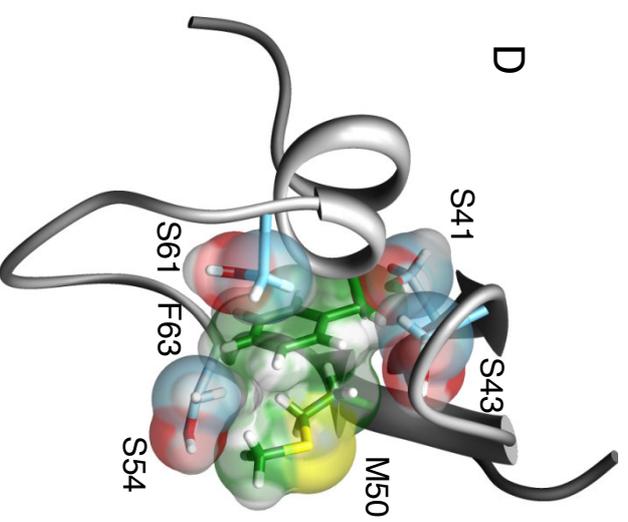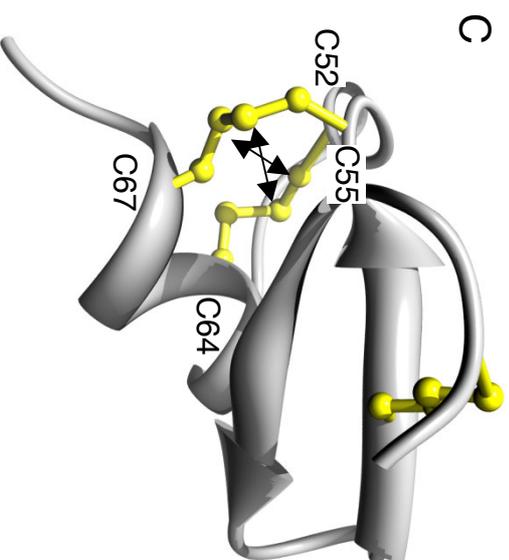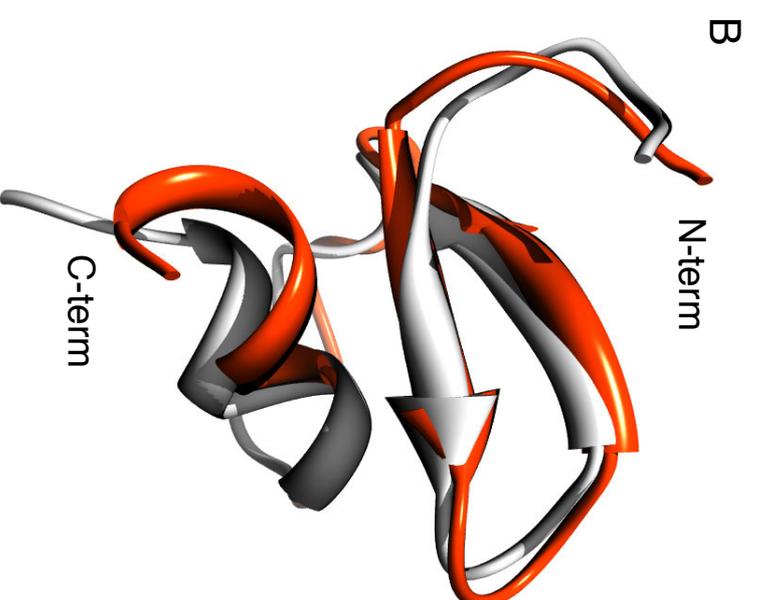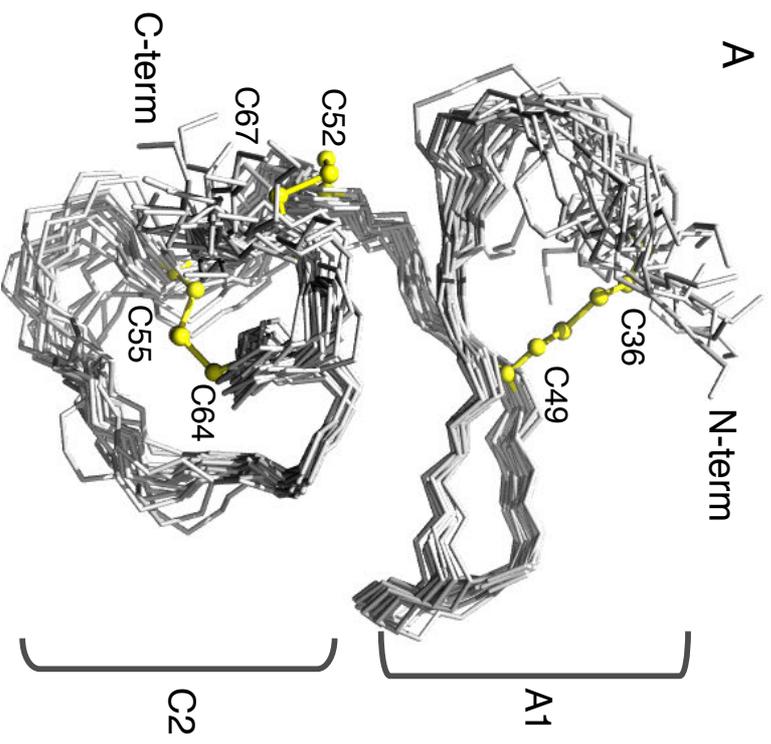
mutant Fn14 was monitored as shown in panel A. The mean fluorescence intensity of TWEAK binding on cells expressing $10^2 - 10^3$ fluorescence units of EGFP (rectangle shown in the first scattergram of panel A) was normalized to the staining intensity obtained with ITEM-4, and plotted as a function of TWEAK concentration. C: Same as panel B, except that the Fn14 mutations were combined with the L46A mutation. D: 293 T cells transfected with full-length wild type Fn14 were stained with the indicated concentration of Flag-TWEAK with the indicated mutations. Only TWEAK mutation Y176A abolished binding to Fn14.  E: Same as panel D, but with Fn14 mutant L46A. The TWEAK mutants K178A, R190A and L192E all failed to interact with Fn14 L46A, which displays a weaker affinity for TWEAK.
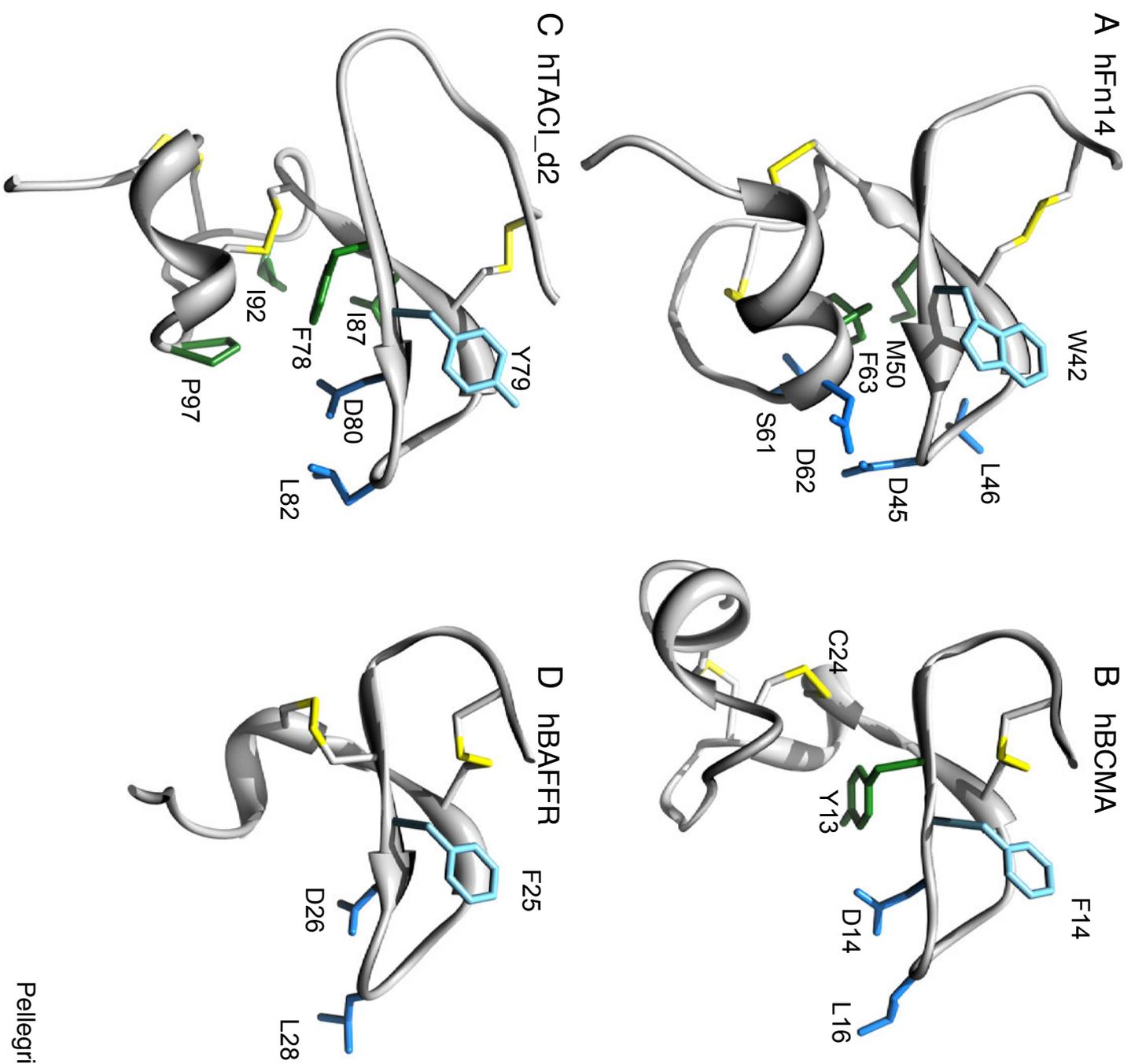
**Figure 6.** Molecular model of the TWEAK-Fn14 complex. A: Residues of hFn14 that were tested in the mutagenesis study. Residues shown in red were critical for ligand binding (in combination with mutation L46A), the residue shown in orange decreased binding, and residues shown in green had no or little effect on ligand binding when mutated to alanine. Residues marked with an asterisk are within 4 Å of TWEAK in the model. Note that residues important for binding are located in both the A1 and C2 modules. B: Model of hFn14 binding to hTWEAK. Residues of both Fn14 and TWEAK that are likely to participate directly in the interaction and whose mutation affects the binding are highlighted (in sticks, green: hydrophobic, red: acidic, blue: basic). The TWEAK trimer is represented in ribbons in shades of gold. Fn14 is in gray ribbon. Fn14 in panels A and B appears rotated approximately 180 degrees, to allow for optimal viewing of the residues described.

Pellegrini et al, Figure 1

A

C-term

C52

C67

C55

C64

N-term

C36

C49

C2

A1

B

N-term

C-term

C

C52

C67

C55

C64

D

S41

S61

F63

S43

S54

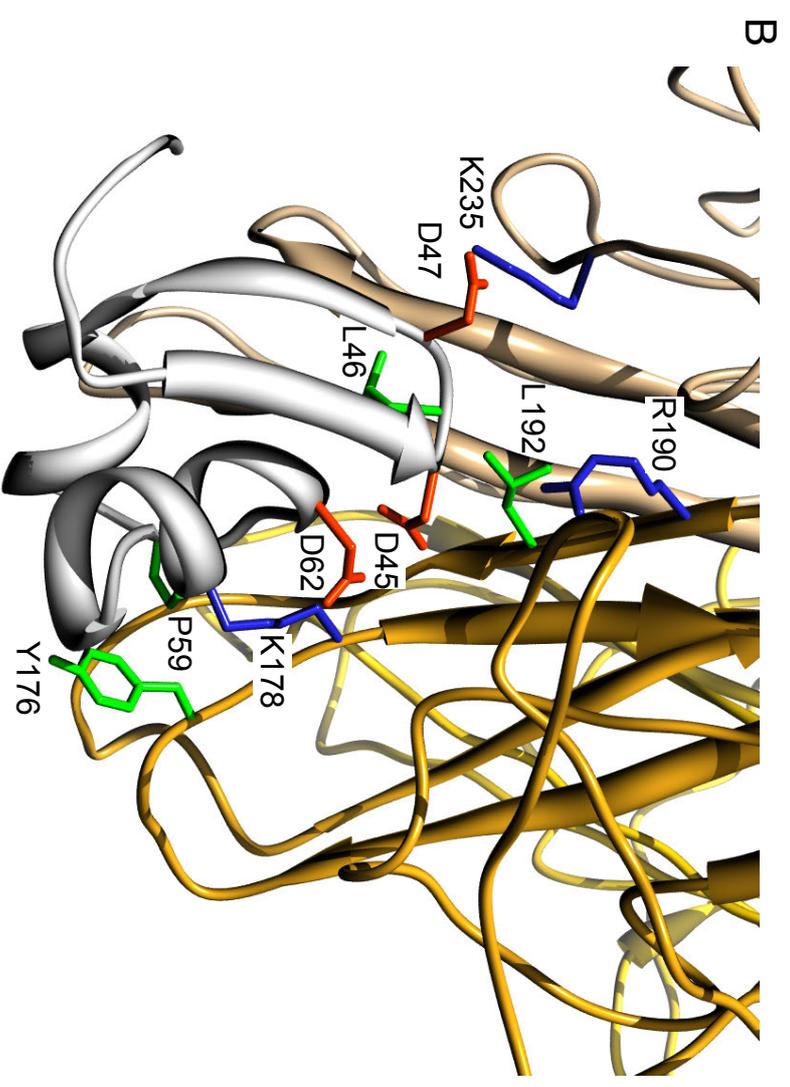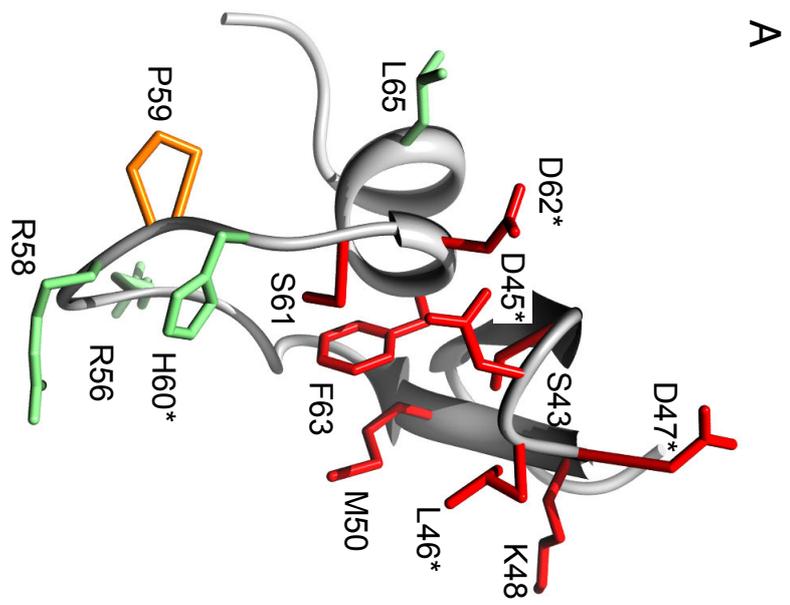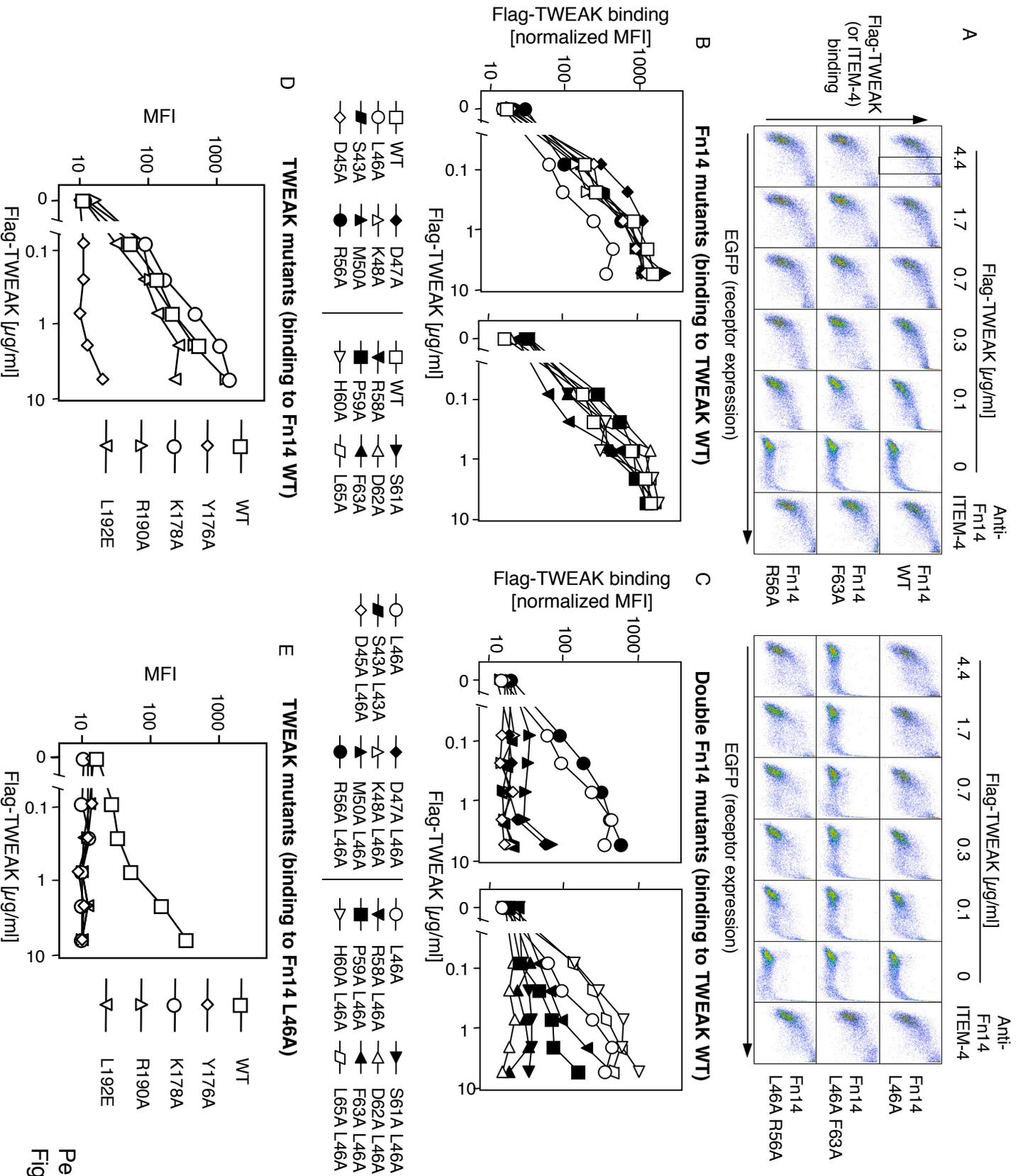M50

Pellegrini et al, Figure 3

A hFn14

B hBCMA

C hTACI_d2

D hBAFFR

Pellegrini et al, Figure 4

Pellegrini et al, Figure 5

A

Flag-TWEAK (or ITEM-4) binding

Flag-TWEAK [μg/ml]

4.4  1.7  0.7  0.3  0.1  0  ITEM-4

Anti-Fn14

EGFP (receptor expression)

Fn14 R56A
Fn14 F63A
Fn14 WT

EGFP (receptor expression)

Flag-TWEAK [μg/ml]

4.4  1.7  0.7  0.3  0.1  0  ITEM-4

Anti-Fn14

Fn14 L46A R56A
Fn14 L46A F63A
Fn14 L46A

B  Fn14 mutants (binding to TWEAK WT)

Flag-TWEAK binding [normalized MFI]

Flag-TWEAK [μg/ml]

□ WT     ◇ D47A     ▽ S61A
○ L46A   △ K48A     ▼ D62A
● S43A   ▲ M50A     ◤ F63A
◇ D45A   ◆ R56A     ◲ L65A

□ WT     ◁ R58A
■ P59A
◢ H60A

C  Double Fn14 mutants (binding to TWEAK WT)

Flag-TWEAK binding [normalized MFI]

Flag-TWEAK [μg/ml]

○ L46A        ◇ D47A L46A     ▽ S61A L46A
● S43A L46A   △ K48A L46A     ▼ D62A L46A
◇ D45A L46A   ◆ M50A L46A     ◤ F63A L46A
              ◢ R56A L46A      ◲ L65A L46A

○ L46A        ◁ R58A L46A
■ P59A L46A
◢ H60A L46A

D  TWEAK mutants (binding to Fn14 WT)

MFI

Flag-TWEAK [μg/ml]

□ WT     ◇ Y176A
○ K178A  △ R190A
▽ L192E

E  TWEAK mutants (binding to Fn14 L46A)

MFI

Flag-TWEAK [μg/ml]

□ WT     ◇ Y176A
○ K178A  △ R190A
▽ L192E

Pellegrini et al,
Figure 6